Mesh Layer Jamming to Cover and Secure Curved Surfaces without Wrinkles

Takashi Mitsuda and Hareruya Tanaka

Mesh layer jamming to cover and secure curved surfaces without wrinkles

Takashi Mitsuda and Hareruya Tanaka

T. Mitsuda is with Ritsumeikan University, College of Information Science and Engineering, Kusatsu-shi, Shiga 525-8577, Japan
(corresponding author; phone: +81-77-561-5068; e-mail: mitsuda@is.ritsumei.ac.jp; ORCID 0000-0002-4647-7387).

H. Tanaka was with Ritsumeikan University, Graduate School of Information Science and Engineering, Kusatsu-shi, Shiga 525-8577, Japan.

Data availability

The data that support the findings of this study are available from the corresponding author upon reasonable request.

Funding

This study was supported by JSPS KAKENHI Grant Number JP22K04019.

Conflict of interest

There are no conflicts of interest to declare.

Mesh layer jamming to cover and secure curved surfaces without wrinkles

Abstract

Layer jamming technologies, which can alter the stiffness of layered sheets enveloped in an elastic bag via internal vacuum pressure, have typically been used for wearable robots. However, wrinkles on the layer jamming element covering a body impair the feeling of wear and are undesirable. Aligning curved surfaces using sheets without wrinkling requires the sheets to be sufficiently elastic, which reduces the stiffness when used for layer jamming. Mesh sheets (i.e., woven fabrics) cannot elongate along the fibers; however, they can elongate and contract in the diagonal direction by changing their shape. This study proposes using mesh sheets for layer jamming and analytically and experimentally demonstrates their ability to fit curved surfaces without wrinkling. The layer jamming element using mesh sheets changes the bending stiffness in proportion to the internal vacuum pressure and the number of sheets, as in conventional layer jamming. The simple structure and flexibility of the mesh layer jamming are not only suitable for fixing a body or fragile objects but also extend the range of applications using layer jamming technologies. This study also provides a foundation for investigating the wrinkle formation associated with curved surface deformation unique to flexible robots.

Keywords

fabric jamming, layer jamming, soft robots, variable stiffness, wearable robots

1. Introduction

The bending stiffness of a laminate of a plastic sheet or paper sealed with an airtight membrane varies with the internal vacuum pressure. When the interior is at atmospheric pressure, the laminated sheets slide against each other and can flexibly bend and deform (see Fig. 1). However, when the internal air is discharged, the pressure difference between the inside and outside of the membrane causes the laminated sheets to adhere to each other. The increased frictional force between the laminated sheets prevents the sheets from sliding, making bending difficult. This variable stiffness mechanism is called layer jamming and has been used to develop wearable force displays (Kawamura et al., 2002), stiffness-controlled robotic manipulators (Kim et al., 2013; Langer et al., 2018; Sadati et al., 2018; Wall et al., 2015; Zuo et al., 2014), shape-changing furniture (Ou et al., 2014), and numerous other applications (Blanc et al., 2017; Fitzgerald et al., 2020).

However, layer jamming is a laminated sheet similar to a notebook, which can be bent in one direction but not in two directions (i.e., it cannot form a curved surface). Forcing it to fit a curved surface causes wrinkling, hindering its applicability (see Fig. 2). For example, when layer jamming is used for securing a living body, the wrinkles can impair the feeling of wear and produce high local contact pressure. Prolonged localized high contact pressure can cause pressure gangrene. In addition, when layer jamming is used for securing a fragile or flexible object, the localized contact pressure can damage the object. If layer jamming consists of elastic sheets such as rubber, it can fit a curved surface without forming wrinkles. However, the bending stiffness of layer jamming depends on the elastic modulus of the sheets in addition to friction (Narang et al., 2018); the bending stiffness of the layer jamming laminated with elastic sheets is smaller than that of the layer jamming laminated with non-stretchable sheets. Accordingly, this study aims to develop a layer jamming that can cover curved surfaces without forming wrinkles to extend its range of applications.

Another variable stiffness mechanism that uses vacuum pressure is particle jamming, in which beads (styrofoam beads or coffee grounds) are placed inside a bag (Blanc et al., 2017; Brown et al., 2010; Fitzgerald et al., 2020; Mitsuda et al., 2002). This bag is flexible, deforms when the interior is at atmospheric pressure, and solidifies when the internal air is expelled. In particle jamming, the particles in the bag can move freely and change into various three-dimensional shapes, including curved surfaces. However, if a variable stiffness element with a thin shape similar to a mat is created with particle jamming, the enclosed particles accumulate downward because of gravity, creating areas with low particle density; the element stiffness is reduced in these areas. To address this problem, a structure that divides particles into small chambers has been proposed (Mitsuda et al., 2003; Steltz et al., 2009). However, this complex structure is labor-intensive to manufacture.

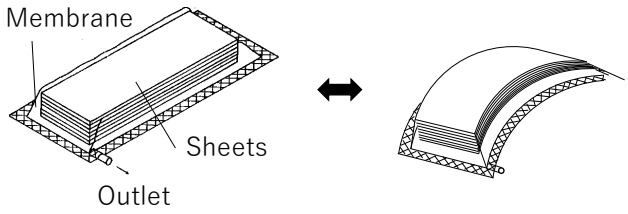

Fig. 1. Layer jamming element. The bending stiffness of layered sheets enveloped in an airtight membrane varies with the internal vacuum pressure. When the internal air is discharged, the pressure difference between the inside and outside of the membrane causes the laminated sheets to adhere to each other. The increased frictional force between the laminated sheets prevents the sheets from sliding, making bending difficult.

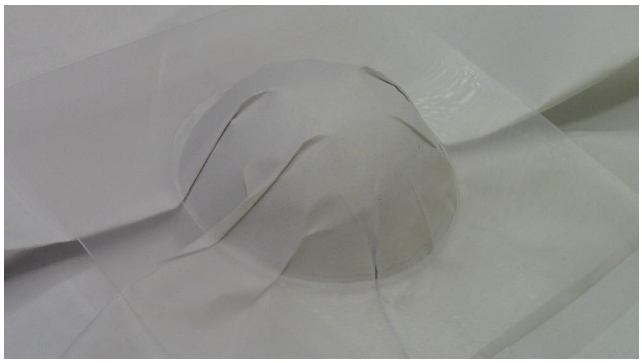

Fig. 2. A view of pressing a copy paper to fit a hemisphere of 60 mm diameter using a polypropylene sheet with a hole. Non-elastic sheets such as paper cannot fit a curved surface without wrinkling.

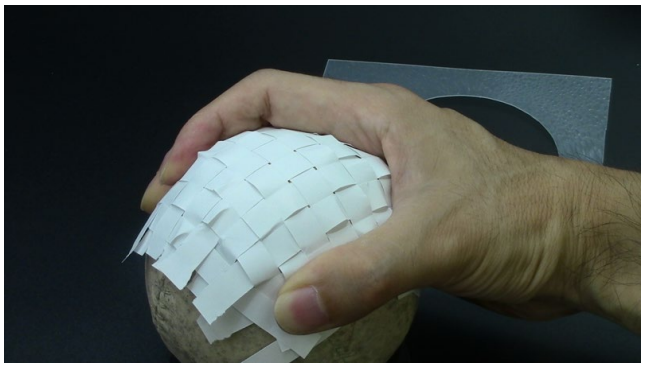

Fig. 3. A view of wrapping a ball of 97 mm diameter with a woven structure of paper strips (width = 10 mm). A woven structure of paper strips fits a curved surface; however, it lifts off the surface when the radius of curvature is small, resulting in gaps.

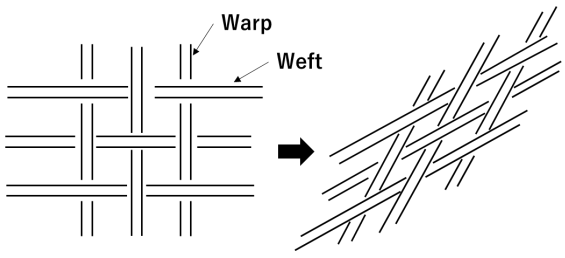

Fig. 4. A plain-weave fabric woven with warp and weft yarns (mesh sheets) can elongate in the diagonal direction of the mesh square but not along the yarns.

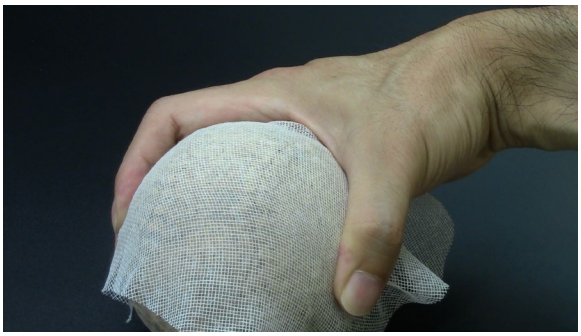

Fig. 5. A view of wrapping a ball of 97 mm diameter with a mesh sheet. A mesh sheet fits a curved surface without wrinkling.

Studies have developed mechanisms to bend a laminated sheet along two directions, whereby the sheets are divided into small segments, similar to fish scales (Kim et al., 2013; Langer et al., 2018; Sadati et al., 2018; Shah et al., 2021; Wall et al., 2015; Zuo et al., 2014). Because these individual sheet segments can slide, laminated segments can elongate or contract and form curved surfaces. However, the individual segments cannot follow a curved surface because they are not elastic, and their size limits the radius of curvature of the resulting deformed surface. In addition, the structure is more complicated to manufacture than conventional layer jamming with sheets. A woven structure with strip-shaped films has also been developed (Matsushita et al., 2020; Ou et al., 2014). However, similar to the fish-scale type, the size of the strip-shaped film limits the curvature of the deformed surface (see Fig. 3). An alternative mechanism that forms a curved surface with the sides of the connected small segment sheets has been developed (Mitsuda and Matsuo, 2005). It offers a wide deformable range and high stiffness; however, its complex structure introduces manufacturing difficulties.

As a thin variable stiffness mechanism that can cover curved surfaces, layer jamming using knitted fabrics from non-stretchable fibers has also been developed (Mitsuda, 2017). The laminated fabrics are highly flexible because of the deformation of the knitting. The laminated fibers adhere to each other when the knit laminate is compressed by removing the internal air, thus inhibiting the knit from stretching and increasing bending stiffness in the laminate. This mechanism has a higher ability to form curved surfaces and is easier to manufacture than conventional layer jamming using sheets with small segments. However, because the knitted fabrics are highly flexible, the stiffness during vacuuming is less than that for conventional layer jamming, as demonstrated in this study.

These observations suggest that layer jamming with a simple structure, high rigidity in a vacuum, and the ability to form curved surfaces without wrinkles is required. In this study, we propose a novel layer jamming that uses laminated mesh sheets (i.e., woven fabrics) instead of knitted or regular sheets. A mesh sheet is a fabric made by horizontally and vertically weaving fibers. Mesh sheets do not change in length in the fiber direction but can stretch and contract in the diagonal direction of the weave, as shown in Fig. 4. Even when the stretchable direction is constrained, curved surfaces can be formed without wrinkling (see Fig. 5)). Although the laminated mesh sheet is less flexible than the knit laminate, it

offers higher bending rigidity in a vacuum. In contrast to the conventional method, mesh layer jamming can serve as a variable-stiffness mechanism to achieve stiffer covers while securing curved surfaces without wrinkles.

The remainder of the paper is organized as follows. Section 2 presents the elasticity of the sheet required to fit curved surfaces without wrinkling and the conditions for the mesh sheet to follow a curved surface. Section 3 presents an experiment in which the mesh sheet and its laminate can fit a hemisphere without wrinkling. The comparison with the conventional layer jamming demonstrates the superiority of mesh layer jamming in covering curved surfaces without wrinkling. Section 4 presents the fitting performance of the mesh jamming for objects of various shapes. Section 5 presents the range of adjustable bending stiffness for layer jamming using the mesh sheet, and Section 6 concludes this study and examines the associated problems.

2. Fitting Ability to Curved Surfaces

2.1. Fitting of Elastic Sheet to Curved Surfaces

Elastic sheets, such as rubber, can fit curved surfaces without wrinkles within the limit of their elongation. In this section, we show the relationship between the elongation ratio of the sheet and a curved surface that is fittable without wrinkles. The proposed mesh layer jamming comprises non-elastic fibers. However, the layered sheets must be enveloped by an elastic sheet that can fit curved surfaces without wrinkles. This analysis can be used to select a membrane and evaluate the applicable range of conventional layer jamming using elastic sheets in wrinkle-free covering applications.

Fig. 6(a) shows a circular sheet of radius r covering a hemisphere of radius r; the sheet stretches uniformly in the radial direction, and a hemisphere with the outer circle of the sheet is located at the equator of the sphere. Most elastic sheets can stretch but cannot contract from their natural length without forming wrinkles. Accordingly, the great circle of the hemisphere (i.e., equator) must be covered by the same or smaller circle on the sheet to prevent wrinkling of the sheet. Fig. 6(a) depicts the case where the circle on the sheet covers the equator with the least stretching. In this case, the line passing through the center of the circle of the sheet (orange line) is elongated and covers the great circle passing through the pole of the sphere (orange circle). The lengths before and after the elongation are respectively $2r$ and πr. Moreover, the elongation ratio of the sheet ((elongated length - original length)/original length) is $(\pi r\text{-}2r)/2r = 0.57$. Thus, elastic sheets with a maximum elongation ratio greater than 0.57 can cover the hemisphere without wrinkles, regardless of the radius of the hemisphere.

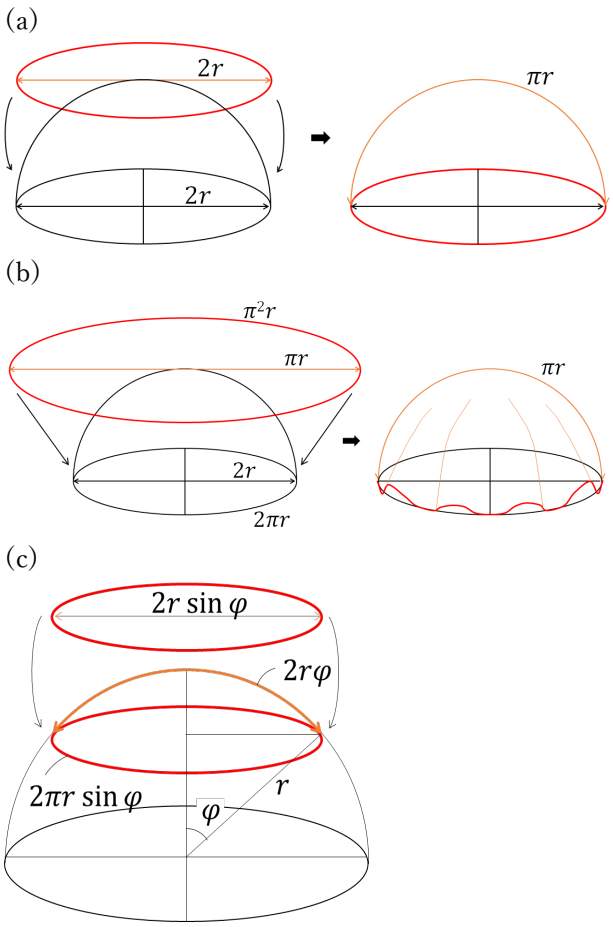

Fig. 6. (a) Sheet radially extended to cover a hemisphere. (b) Sheet not extended to cover a hemisphere. (c) Sheet radially extended to cover part of a sphere.

Next, we consider a hemisphere with radius r with a circular sheet covering it without stretching, as shown in Fig. 6(b). In this case, the diameter of the circular sheet is πr, which is equal to half the length of the great circle passing through the pole of the hemisphere. The circumference of the outer circle of this circular sheet is $\pi^2 r$, which is longer than the length of the equator of the hemisphere $2\pi r$. Accordingly, the remainder of the outer circle on the sheet causes wrinkles. In other words, the excess of the circumference of the sheet causes wrinkles when a hemisphere is covered with a non-elastic sheet.

The portion of spherical surfaces that a sheet can fit without wrinkles is determined by the elongation ratio of the sheet. As shown in Fig. 6(c), a line segment passing through the center of the sphere forms an angle φ with the line connecting the center of the sphere and the pole. The length of the small circle on the sphere formed by rotating the line segment around the line connecting the center of the sphere and the pole is $2\pi r \sin\varphi$. Therefore, the diameter of the circular sheet is $2r \sin\varphi$ when it is stretched in the radial direction and covers a part of the hemisphere above the small circle without wrinkles. The arc length of the great circle passing through the pole in the circular sheet covering the sphere is $2r\varphi$. Therefore, the elongation ratio of this sheet γ is expressed as

$$\gamma = \frac{2r\varphi - 2r\sin\varphi}{2r\sin\varphi} = \frac{\varphi - \sin\varphi}{\sin\varphi} . \quad (1)$$

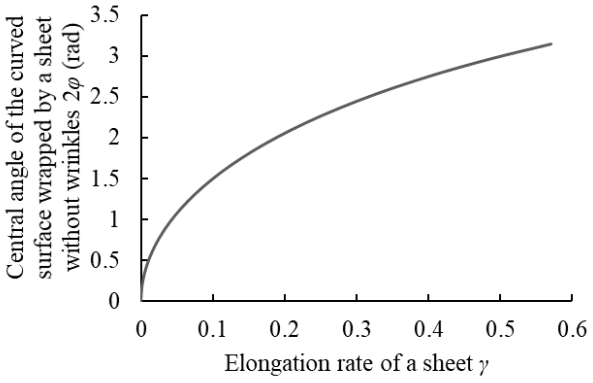

Fig. 7. Relationship between sheet elasticity γ and the central angle 2φ of the spherical area that can be covered without wrinkles. When the elongation rate of a sheet γ is 0.57, the central angle 2φ is π. Therefore, the sheet can cover the entire hemisphere without wrinkling. The portion of the hemisphere that can be covered without wrinkles decreases with the decreasing elongation rate of a sheet.

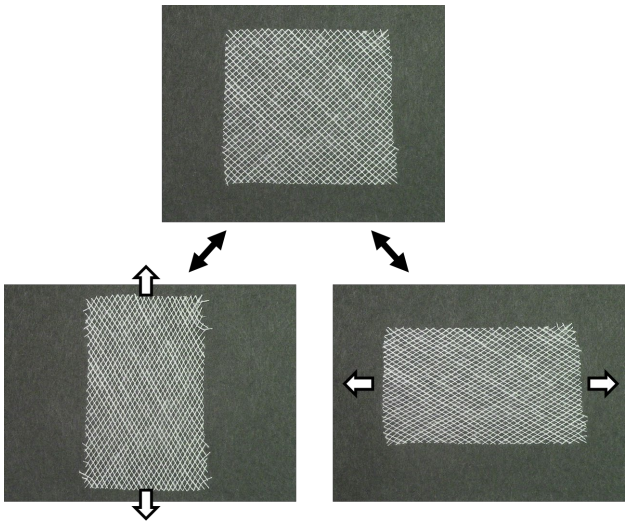

Fig. 8. Skewing of a mesh sheet. When the mesh sheet is stretched in a diagonal direction of the mesh square, it is shortened in the orthogonal direction.

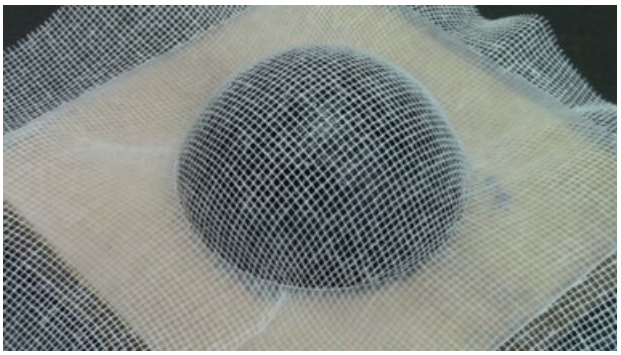

Fig. 9. Mesh sheet fitting to a hemisphere of 60 mm diameter without wrinkling. Pressing the mesh sheet using a polypropylene sheet with a hole fits the mesh sheet to the hemisphere without wrinkling.

The central angle 2φ of the spherical surface along which the sheet can be fitted without wrinkles is determined from the maximum elongation ratio of the sheet γ. Fig. 7 shows the relationship between the elongation ratio of the sheet and the central angle of the sphere calculated using Eq. (1). When the elongation rate of a sheet γ is 0.57, the central angle 2φ of the spherical area that can be covered without wrinkles is π. Therefore, as described previously, the sheet can cover the entire hemisphere without wrinkling. The portion of the hemisphere that can be covered without wrinkles decreases with the decreasing elongation rate of a sheet. According to Eq. (1), the elongation ratio of the sheet, and not the radius of curvature, determines the portion of the curved surface that can be fitted without wrinkling. If the sheet is not elongated (i.e., elongation ratio = 0), wrinkles will always occur when the sheet is fitted to a spherical surface, even if the curvature is small.

This analysis holds for the case where the elastic sheet is stretched uniformly in radial directions to cover the spherical surface. Moreover, this analysis neglects the orthogonal shrinkage of the sheet when the sheet is stretched. Uneven stretching should not reduce the elongation rate of a sheet required to cover curved surfaces without wrinkling. However, the analysis considering the orthogonal contraction of a sheet due to stretching requires a complex numerical simulation. Accordingly, we experimentally examined the analysis described in this section.

A natural rubber sheet (thickness = 14 mm), which is the same as the membrane of the mesh layer jamming sheet developed in this study, was placed over a sphere of 50 mm diameter. We stretched the sheet by hand with as little force as possible to cover the hemisphere without wrinkling. We marked the hemisphere's equator and then returned the sheet to its original flat surface to measure the diameter of the mark. We performed five measurements.

The marks were almost regular circles; the average length of the short axis was 51.2 (SD = 2.2) mm; the difference between the length of the long and short axes of the circle was 2.4 mm on average. The elongation rate calculated with the short axis' length was 0.54 (SD = 0.07), which was similar to the theoretical value (0.57). We also conducted uneven stretching of the sheet; however, the lengths of the short axis of the marks did not increase. Therefore, the analysis described in this section roughly estimates the elongation rate of a sheet to cover a hemisphere.

As described previously, a non-stretchable sheet cannot fit on any spherical surface regardless of the curvature. However, sheets that cannot be stretched in some directions and shortened along others, such as the mesh sheet, can fit a spherical surface without wrinkles, as described in the next section.

2.2 Fitting of Mesh Sheet to Curved Surfaces

A plain-weave fabric woven with warp and weft yarns is hereinafter referred to as a mesh sheet. The mesh deforms into a diamond shape, with one diagonal elongated and the other

shortened when the mesh sheet is stretched in the diagonal direction of the mesh square, as shown in Figs. 4 and 8. The deformation of the mesh is referred to as skewing (Mack and Taylor, 1966; Moriguchi and Sato, 1972; Shinohara and Uchida, 1972). This deformation is different from skewing in the field of strength of materials. This skewing of the meshes allows the sheet to fit curved surfaces without wrinkles, even when its fibers are not elongated. Fig. 9 shows an example of a mesh sheet made of polyester fibers that fits a hemisphere. In this example, the meshes are elongated in the longitudinal direction and contracted in the latitudinal direction. The fiber and weave control the amount of skewing of the mesh. Generally, the coarser the weave, the greater the skewing of the mesh sheet. However, even a woven fabric in which the meshes are not visible can cover curved surfaces to a certain extent without wrinkling, as in a Furoshiki (i.e., Japanese wrapping cloth) or a garment.

Moriguchi (1947) and Mack and Taylor (1956) performed a theoretical analysis of the fitting of woven fabrics to curved surfaces using different approaches. Moriguchi analyzed the case of wrapping a sphere by pulling the four corners of a square sheet made of woven fabrics. Mack and Taylor (1956) analyzed the case where the top and bottom edges of a cylinder made of woven fabrics were squeezed to align it with a sphere. In both studies, the conditions for the fabric to follow a curved surface were expressed using differential equations. Shinohara and Uchida (1966) integrated these studies, and Moriguchi and Sato (1972) comprehensively re-analyzed the work of Moriguchi. The following paragraphs provide an example from the analysis conducted by Moriguchi and Sato (1972).

Equation (2) is satisfied for the warp and weft crossing angles when a curved surface is wrapped with a mesh sheet under the following assumptions: the thickness of the yarn is not considered, there is no yarn elongation, and the curve of the yarn on the surface coincides with the geodesic line of the surface.

$$K = \frac{-1}{\sqrt{EG - F^2}} \frac{\partial^2 \theta}{\partial x \, \partial y} \tag{2}$$

Here, x and y are the coordinates of the curve along the warp and weft, θ is the intersection angle of the weft and yarns, E, G, and F are the coefficients of the fundamental form of a surface, and K is the Gaussian curvature. When the warp and weft are not extending, we can set $E = G = 1$ and $F = \cos\theta$. Therefore, the above equation is simplified to

$$\frac{\partial^2 \theta}{\partial x \, \partial y} + \frac{\sin\theta}{K} = 0. \tag{3}$$

Nondimensionalizing Eq. (3) with

$$\frac{xy}{r^2} = t, \tag{4}$$

Eq. (3) becomes

$$t\frac{d^2\theta}{dt^2} + \frac{d\theta}{dt} = -\sin\theta\,. \tag{5}$$

Consider the case of wrapping a sphere by pulling the four corners of a square fabric with both sides along the warp and weft yarns and placing the origins of the weft and warp ($x = 0$, $y = 0$) at the poles of the sphere. The boundary conditions in this case are $\theta = \pi/2$ and $\theta' = 1$ at $t = 0$. Solving Eq. (5) with these boundary conditions, the crossed angle θ of the warp and weft yarns can be approximated using Eq. (6).

$$\theta \approx \frac{\pi}{2} - t + \frac{t^3}{18} \tag{6}$$

Fig. 10 shows the relationship between the intersection angle and the coordinates of the curve along the warp and weft. In the meridian directions along warp and weft ($y = 0$ or $x = 0$), $\theta = \pi/2$, indicating that the mesh is not skewed. However, in the diagonal direction of the mesh (i.e., $x = y$), θ decreases, and skewing of the meshes is required to fit a curved surface. The portion of surfaces that can be fitted by the mesh sheet without wrinkling is determined by the range of skewing of the mesh. Theoretically, a hemisphere with radius r can be fitted by a sheet whose shape is a rounded square with diagonals of πr when the minimum skewing angle of the mesh sheet is less than 0.64 (37°), which has been experimentally verified.

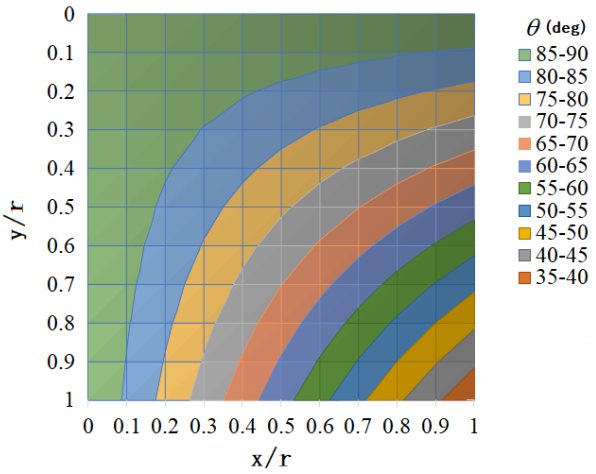

Fig. 10. Relationship between intersection angle and curve coordinates along the warp and weft.

The minimum skewing angle of the mesh sheet used in this study is 32°, which can theoretically fit into a hemisphere without wrinkles (details of the mesh sheet are shown in the next section). Fig. 11(a) shows the mesh sheet fitted to the hemisphere in Fig. 9, with latitude and longitude lines drawn in 30° and 45° increments, respectively. The diagonal direction of the square corresponded to that of the warp and weft yarns, whose length of 78 mm coincided with the circumferential length through the poles of the hemisphere (25 mm radius). Thus, the warp and weft yarns were negligibly stretched. The length of the sides of the square was 67 mm, which was shorter than the circumference of the hemisphere. Therefore, the mesh sheet elongated an average of 1.16 times (i.e., 78 mm/67 mm) in the direction of the side of the square, indicating that the meshes were skewed. Fig. 11(b) presents a magnified view of the deformation of the mesh sheet. The skewing of the mesh increases as one moves away from the hemispherical poles, which is consistent with the results of the theoretical analysis.

The direction of the warp and weft yarns of the mesh sheet fitted to the hemisphere is the direction of the diagonals of the drawn square. Accordingly, when making a square laminated sheet, it is better to have the sides of the sheet parallel to the diagonals of the mesh rather than parallel to the direction of the yarns, such that the laminated sheet can follow a wider curved surface.

(a)

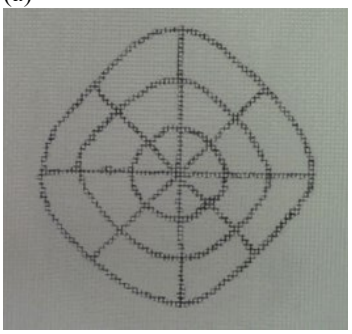

(b)

(c)

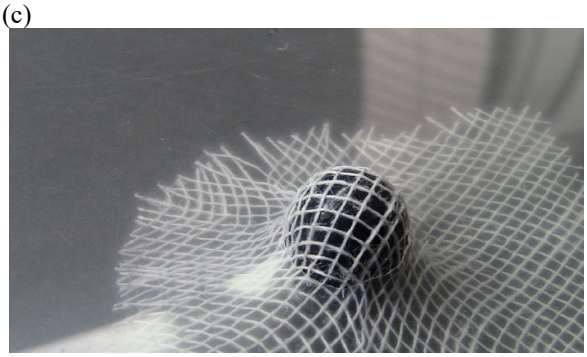

(d)

Fig. 11. (a) Mesh sheet fitted to a hemisphere with latitude lines drawn in 30° increments and longitude lines drawn in 45° increments. (b) Magnified view of mesh sheet fitted to a hemisphere. (c) Wrapping a hemisphere of 10 mm diameter with a mesh sheet. (d) Wrapping the top of a rectangular pillar (40 × 40 × 80 mm).

Eq. (6) indicates that the mesh can cover a hemisphere regardless of size. This analysis neglects the yarn thickness and the mesh size. However, as shown in Fig. 11 (c), the mesh can cover a small sphere of 10 mm diameter.

The analysis for curved surfaces other than spheres is challenging because the Gaussian curvature varies depending on the position on the surface. Moreover, the analysis of polyhedrons or surfaces containing edges is challenging for a similar reason. As shown in Fig. 11 (d), the mesh can cover the top of a rectangular prism and the corners without wrinkling. However, the theoretical investigation of its effective range is beyond the scope of this study. Therefore, we show the shapes that mesh layer jamming can fit without wrinkling experimentally in Section 4.

3. Fitting ability of mesh sheet and laminate to a hemisphere

As previously mentioned, a sufficiently skewed mesh sheet can cover the hemisphere without wrinkling. However, stretching the sheet in the appropriate directions is necessary for skewing the meshes. Not all sheets are properly stretched when mesh sheets are laminated. Therefore, we experimentally investigated the portion of curved surfaces that can be covered without wrinkles when a laminate of mesh sheets on a hemisphere is pressed down. In addition, we examined if non-stretchable sheets could cover curved surfaces to confirm the advantage of the mesh sheets.

3.1 Experimental Method

The mesh sheet was made of a plain weave (weave pitch of 1.2 mm) of twisted polyester fibers (diameter = 0.2 mm). The minimum skewing angle of the mesh sheet was 32°. For the non-stretchable sheets, we employed copy papers (thickness = 0.1 mm) and polypropylene sheets (thickness = 0.17 mm). We cut each sheet into squares of 10 cm per side and placed them on an inked hemisphere with a diameter of 50 mm. Then, we placed a rubber ring with a circular hole with an inner diameter of 45 mm over the sheet and pressed it down. Fig. 12 shows that the sheet was pressed against the hemisphere and inked. The flexibility of the rubber ring allowed the sheet to cover the hemisphere while stretching in the radial direction. Subsequently, we removed the rubber ring and sheet from the hemisphere and returned the sheet to its original flat surface to observe the inked area. We performed three measurements for each sheet. The same experiment was performed with 8, 16, and 32 sheets stacked on top of each other for the mesh sheets. The experiment using eight sheets was performed for both copy papers and polypropylene sheets.

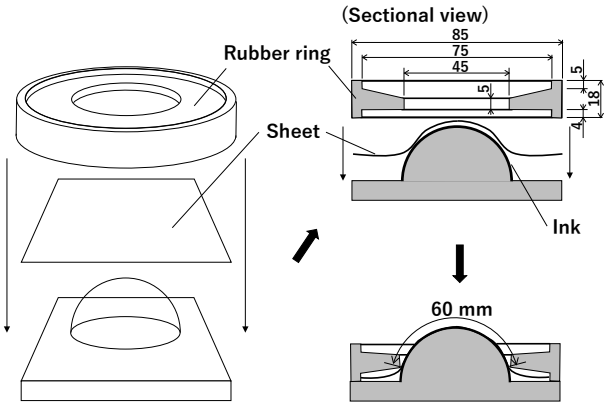

Fig. 12. Pressing a sheet onto a hemisphere with a rubber ring.

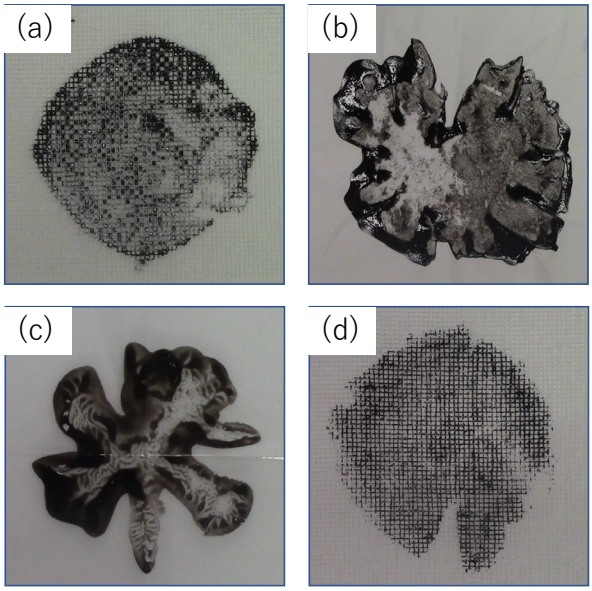

Fig. 13. Area of ink on the sheet pressed against a hemisphere. (a) Mesh sheet; (b) copy paper; (c) polypropylene sheet; and (d) 32 mesh sheets. A mesh sheet covered a hemisphere without wrinkling. In contrast, a copy paper and polypropylene sheet covered only a small area on the top of the hemisphere. When 32 mesh sheets were stacked, the periphery developed a small wrinkle.

The inner hole of the rubber ring in contact with the hemisphere was 4 mm above the bottom surface of the rubber ring. Therefore, the sheet or the laminated sheet entered the gap when we pressed the rubber ring against the hemisphere. The contact area of the rubber ring is bent slightly upward when pressed against the hemisphere. Therefore, the sheet held down by the rubber ring was in the hemispherical region approximately 10 mm above the bottom surface, and the circumference through the poles of this spherical region was approximately 60 mm.

3.2 Results

Fig. 13 shows an example of ink adhering to a mesh sheet, copy paper, polypropylene sheet, and 32 laminated mesh sheets. The mesh sheet covered a spherical surface without wrinkling in all trials. The area where the ink adhered had a rounded square shape (Fig. 13(a)), which is consistent with the theoretical analysis results. The diagonal direction of the square coincided with the fiber direction of the mesh such that it did not stretch when pressed against the spherical surface. The length of the diagonal of the square was 58 mm in all three trials, matching the length of the spherical area pressed down by the rubber plate, which confirmed that the fibers did not stretch nearly as much. For all three trials, the side of the square was 50 mm in length. Therefore, the sheet was stretched 1.16 times (58/50 = 1.16 times) on average in the diagonal direction of the mesh.

By contrast, for the copy paper (Fig. 13(b)) and polypropylene sheet (Fig. 13(c)), the only spherical area covered without wrinkles in all three trials was near the pole of the hemisphere, resulting in multiple distinct wrinkles. In each trial, the diameters of the circles inscribed in the inked areas were 24, 14, and 14 mm (average 17 mm) for the copy paper and 6, 14, and 20 mm (average 13 mm) for the polypropylene sheets.

When 8 or 16 mesh sheets were stacked on top of one another, the periphery developed small wrinkles, but the majority of the hemisphere was smooth. The diameters of the circles inscribed in the inked area in the trials were 48, 48, and 48 mm (average 48 mm) for the 8 mesh sheets and 48, 50, and 44 mm (average 47 mm) for the 16 mesh sheets. Wrinkles were noticeable when 32 mesh sheets were stacked (Fig. 13(d)). The diameters of the inscribed circles in each trial were 34, 28, and 30 mm (average 31 mm). The wrinkles may have occurred because the force to stretch the sheet was not generated by simply pressing the top surface of the laminate, and the weave was not sufficiently sheared and deformed. However, even in this case, the sheet followed a wider spherical area than a single sheet of copy paper or polypropylene. The polypropylene sheet and eight sheets of copy paper developed stiff wrinkles, and the rubber ring could not be pushed to the bottom of the hemisphere.

4. Fitting Performance

Fig. 14 shows the vacuuming of the layer jamming element, consisting of 16 mesh sheets covered with natural rubber, to -75 kPa to maintain the shape after it is fitted to the hemisphere used in the previous experiment. It shows that the laminated sheets followed the sphere without wrinkling and maintained their shape when covered with an outer membrane.

We also examined the fitting performance of objects of various shapes. Fig. 15 shows the target objects and the hardened mesh jamming sheets obtained via internal air discharge after wrapping. The mesh jamming sheets were able to wrap balls of 97, 65, and 40 mm diameters and a hemispherical cap of 10 mm diameter. This confirms that they can fit a hemisphere of any size. Moreover, they were able to wrap an egg-shaped ball (long axis 45 mm), a rectangular pillar (40 × 40 × 80 mm), a triangular prism (79 × 77 × 110 mm, height = 39 mm), and a leg of a children's doll, which indicates that the mesh jamming sheets can wrap objects of various shapes, even if they have edges.

As shown in Fig. 14 and 15, the mesh sheet did not wrinkle, while the outer membrane, natural rubber, wrinkled around the

target objects. These wrinkles are not a problem because they appear only on the periphery of the targets; these wrinkles can be excluded by stretching the outer membrane because natural rubber is stretchable in all directions. A thicker outer membrane may cause fewer wrinkles; however, selecting the outer membrane and appropriate covering (i.e., stretching) method require further investigation.

Fig. 14. Hemisphere covered by mesh layer jamming sheets (16 sheets). The laminated sheets followed the sphere without wrinkling and maintained their shape by discharging the internal air.

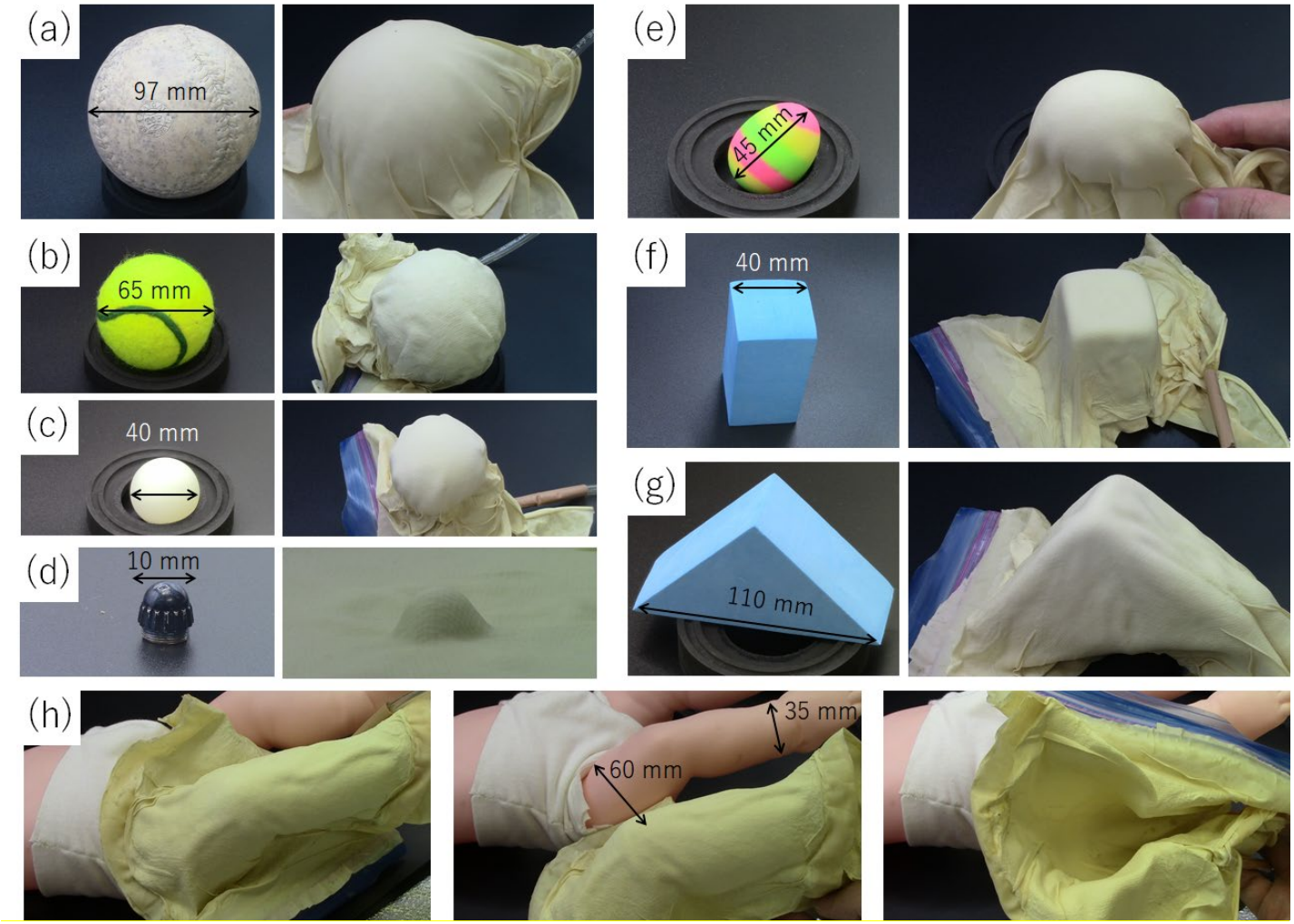

Fig. 15. Wrapping performance of the mesh jamming sheets (16 sheets). Spheres with diameters of (a) 97 mm, (b) 65 mm, and (c) 40 mm. (d) Hemispherical cap of 10 mm diameter. (e) Egg-shaped ball (long axis = 45 mm). (f) Rectangular pillar (40 × 40 × 80 mm). (g) Triangular prism (79 × 77 × 110 mm, height = 39 mm). (h) Leg of a children's doll. The mesh jamming sheets can wrap objects of various shapes even if they have edges.

5. Bending Stiffness of Mesh Layer Jamming Elements

We investigated the effect of the number of laminated sheets and the internal vacuum pressure on the bending stiffness to examine the adjustable range of bending stiffness of layer jamming with mesh sheets.

5.1 Experimental Method

We measured the bending stiffness of a layer jamming element by layering the mesh sheets (width = 20 mm and length = 70 mm) and enveloping them in a natural rubber bag (thickness of 0.14 mm). The fibers of the mesh sheets were parallel along the width and length. We measured the bending stiffness using a universal testing machine (IMADA, MX2-500 N) with an attached force gauge (IMADA Corporation, ZTA-20 N). As shown in Fig. 16, measurements were obtained using a three-point bending flexural test in which a layer jamming element placed on supporting pins with a spacing of 64 mm was pressed down at a speed of 50 mm/min using an indenter whose cross-section had a semicircle with a radius of 6 mm. The number of mesh layers in the measured elements was 8, 12, 16, 24, and 32, with respective thicknesses (including the outer film) of 1.9, 2.5, 3.5, 5.0, and 6.5 mm. The bending stiffness was measured at six different vacuum pressures: 0, -10, -20, -40, -60, and -75 kPa. We obtained three measurements for every 30 combinations of five types of laminations and six types of internal vacuum pressure.

Fig. 16. A three-point bending flexural test in which a layer jamming element placed on supporting pins with a spacing of 64 mm was pressed down at a speed of 50 mm/min using an indenter whose cross-section has a semicircle with a radius of 6 mm.

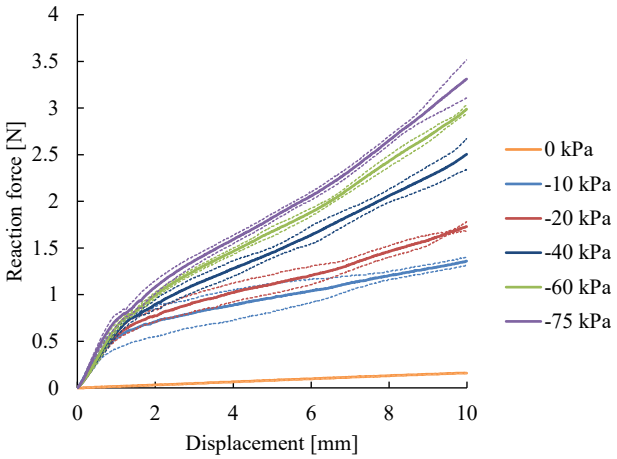

Fig. 17. Bending stiffness of the mesh layer jamming element with 16 layered sheets at different internal vacuum pressures (the solid line shows the mean value, and the dashed line shows the standard deviation). Similar to layer jamming with paper and polypropylene sheets, the stiffness increased as the vacuum pressure increased.

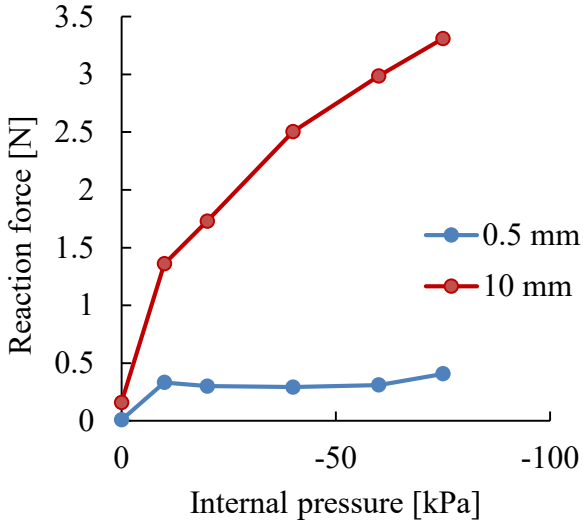

Fig. 18. Relationship between internal vacuum pressure and bending stiffness. The stiffness for small displacements (0.5 mm) hardly changes with internal vacuum pressure, except when the interior is at atmospheric pressure (0 kPa). In contrast, there is a linear relationship between the internal vacuum pressure and stiffness for large displacements (10 mm).

Additionally, for comparison with mesh layer jamming, the bending stiffnesses of the paper and knit layer jamming elements were measured. The number of paper and knit layers were 32 and 80, respectively, which were determined such that the thickness equals the mesh layer jamming element with 16 layered sheets when vacuumed. We employed the copy paper (thickness of 0.1 mm) described in Section 3 for the paper layers. A plain knitted polyester (thickness of 0.04 mm) was used for knit layers. Further, we measured the bending stiffness of 16 mesh laminates with warp and weft yarns inclined at 45 degrees to the long axis of the sheet to investigate the effect of fiber direction on mesh layer jamming. We enveloped all the laminates in a rubber bag same as the normal mesh layer jamming elements. We took the measurements three times each for these elements at a vacuum

(-75 kPa) and internal atmospheric pressure.

5.2 Results

Fig. 17 shows the bending stiffness of 16 layered sheets at each internal vacuum pressure. Similar to layer jamming with paper and polypropylene sheets, the stiffness increased as the vacuum pressure increased. Consistent with previous studies (Kawamura et al., 2002; Narang et al., 2018), the reaction force rapidly increased at small displacements, after which the increase in the reaction force with displacement (slope of the graph) became smaller. Narang et al. (2018) suggested that when the load was small, the sheets adhered to each other and deformation occurred because of the elasticity of the sheets; whereas, for large loads, deformation occurred because of the sliding between the sheets. In this study, the magnitude of the reaction force against displacement is called stiffness, which is different from the stiffness in the field of material strength. The displacement is proportional to the load for elastic materials, such as metals. The displacement returns to zero when the load is removed if the displacement is not too large. However, in layer jamming, the slip between sheets and elastic deformation of the sheets determine the relationship between load and displacement. The displacement does not return to zero, and strain remains when the load is removed, similar to particle jamming.

Fig. 18 shows the relationship between the reaction force and the internal vacuum pressure at displacements of 0.5 and 10 mm. The stiffness for small displacements hardly changes with internal vacuum pressure, except when the interior is at atmospheric pressure (0 kPa). In contrast, there is a linear relationship between the internal vacuum pressure and stiffness for large displacements. This result is similar to that of previous studies on layer jamming (Kawamura et al., 2002; Narang et al., 2018). In mesh layer jamming, as in other vacuum-type variable stiffness elements, the stiffness can be modulated by the internal vacuum pressure.

Fig. 19 shows the bending stiffness at an internal vacuum pressure of -75 kPa for different numbers of mesh sheets. Fig. 20 shows the relationship between the reaction force at a displacement of 10 mm and the number of sheets. In layer jamming with mesh sheets, the bending stiffness had a linear relationship with the number of sheets, similar to that in layer jamming with polypropylene sheets or paper. Compared to previous studies (Kawamura et al., 2002; Narang et al., 2018) for conventional layer jamming, the present experiments with a diverse number of sheets and internal vacuum pressure clearly showed the linearity between the number of sheets and stiffness.

Fig. 21 shows the bending stiffness for knit, mesh, and paper layer jamming elements. As expected, the bending stiffness of mesh layer jamming was greater than that of knit layer jamming; however, it is smaller than that of paper layer jamming. The bending stiffness for the mesh layer jamming element, whose fibers inclined 45 degrees to the long axis of the sheets, was smaller than that of the mesh layer jamming element whose fibers were along the edges of the sheets. This difference in bending stiffness with fiber direction requires further investigation.

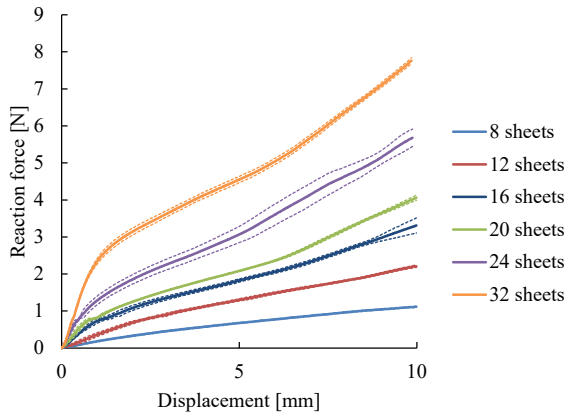

Fig. 19. Relationship between bending stiffness, number of sheets, and internal vacuum pressure (solid line indicates the mean value; dashed line indicates the standard deviation).

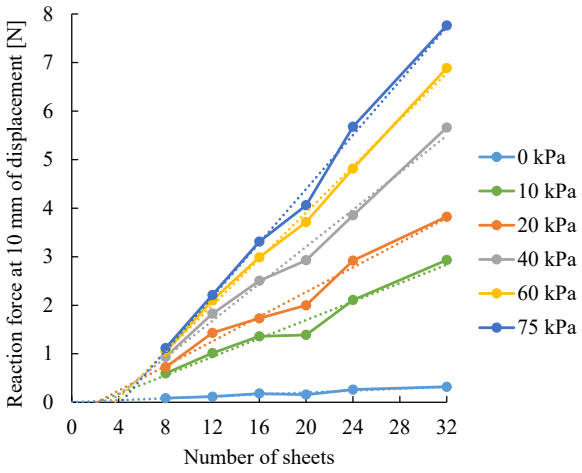

Fig. 20. Relationship between bending stiffness, number of sheets, and internal vacuum pressure. In layer jamming with mesh sheets, the bending stiffness had a linear relationship with the number of sheets, similar to that in conventional layer jamming.

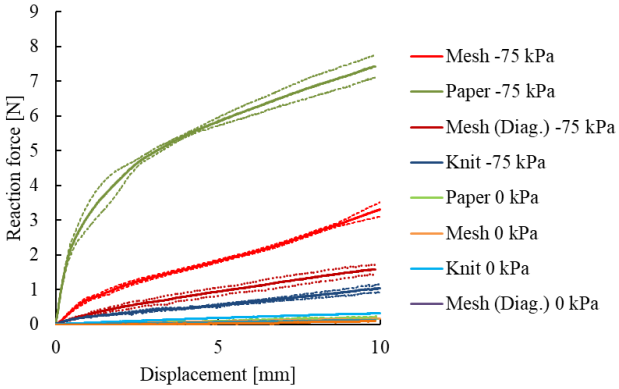

Fig. 21. Bending stiffness of paper, mesh, and knit layer jamming elements at vacuum (-75 kPa) and internal atmospheric pressure. Mesh (Diag.) shows the bending stiffness of the mesh layer jamming element whose fibers are diagonal to the long axis of the sheets (the solid line shows the mean value, and the dashed line shows the standard deviation). The bending stiffness of mesh layer jamming was greater than that of knit layer jamming; however, it is smaller than that of paper layer jamming.

6. Conclusion

In this study, we developed a novel layer jamming by layering mesh sheets that can follow curved surfaces without wrinkles. After analytically determining the relationship between the portion of curved surfaces that can be covered by elastic sheets without wrinkles and the elasticity of the sheets, we experimentally verified the portion of curved surfaces that layer jamming can cover without forming wrinkles. The results indicated that the mesh layer jamming could fit hemispheres regardless of size. It could follow objects of various shapes even when they had edges. This versatile fitting performance extends its applicability.

The bending stiffness of mesh layer jamming increased linearly as the number of sheets increased; it was approximately proportional to the internal vacuum pressure, as in conventional sheet-based layer jamming. The bending stiffness of mesh layer jamming was higher than that of knit layer jamming but was lower than that of paper layer jamming. We compared the bending stiffness for the same total thickness in a vacuum. However, comparisons under different conditions are required because several differences exist between the mesh and knit layer jamming. For example, knit layer jamming is soft and fluffy at atmospheric pressure. Mesh layer jamming is flexible; however, it feels similar to paper layer jamming to the touch. Therefore, the force required to cover curved surfaces would be less for knit layer jamming. Knit layer jamming or its combination with mesh layer jamming may be more suitable in some uses where thickness is not critical because increasing the thickness increases the bending stiffness. In addition, the mechanical properties and fabrication efforts of both types of layer jamming will depend on the fiber type, thickness, and pitch of the knit. In future work, the mechanical properties of knit and mesh layer jamming and the combinations will be investigated to achieve fabric jamming enhancements.

Next, we discuss the applications and limitations of mesh layer jamming. Mesh layer jamming can be used to cover curved biological surfaces and fragile objects of various shapes without gaps, fixing the shape or protecting the surface because it can follow the edges of objects and curved surfaces with a small radius of curvature that cannot be followed by conventional layer jamming. It can also wrap around multi-degree-of-freedom joints of living bodies and robots to adjust their stiffness or constrain their movement. It can also be used as a device for attaching an object to a living body, such as a wearable robot or head-mounted display. It is expected to have a variety of applications, such as an object that can be reshaped.

However, several problems require solutions for practical use. The first is the compatibility of flexibility and durability of the outer membrane. The flexibility of the outer membrane is essential to cover the object without wrinkles with a small force; however, flexible materials are generally less durable. Therefore, striking a balance between flexibility and durability, depending on the application, is required. The second is to achieve both deformation flexibility and high rigidity after discharging the internal air. Increasing the thickness of mesh jamming sheets can increase the bending stiffness; however, the thicker the sheets, the lower the deformation flexibility. The required balance between flexibility and rigidity depends on the application. The third is to reduce the force applied to the target object during wrapping. Stretching the mesh sheets and wrapping them around the object while keeping the contact force between the mesh sheet and the object requires skill. In applications where the contact force with the object is regulated, an auxiliary device for wrapping may be required.

Collectively, this study provides a novel vacuum-type variable stiffness mechanism and a foundation for investigating the mechanism of wrinkle formation associated with curved surface deformation unique to flexible robots.

Acknowledgements

Conflicting Interests

The authors have no conflicts of interest to declare.

Data Availability

The data that support the findings of this study are available from the corresponding author upon reasonable request.

References

Aktaş B, Narang YS, Vasios N, Bertoldi K and Howe RD (2021) A modeling framework for jamming structures. *Advanced Functional Materials* 31(16): 2007554.

Blanc L, Delchambre A and Lambert P (2017) Flexible medical devices: Review of controllable stiffness solutions. *Actuators* 6(3): 23.

Brown E, Rodenberg N, Amend J, Mozeika A, Steltz E, Zakin MR, Lipson H and Jaeger HM (2010) Universal robotic gripper based on the jamming of granular material. *PNAS* 107(44): 18809–18814.

Fitzgerald SG, Delaney GW and Howard D (2020) A review of jamming actuation in soft robotics. *Actuators* 9(4): 104.

Kawamura S, Yamamoto T, Ishida D, Ogata T, Nakayama Y, Tabata O and Sugiyama S (2002) Development of passive elements with variable mechanical impedance for wearable robots. In: *Proceedings 2002 IEEE international conference on robotics and automation*, 11–15 May 2002, pp. 248–253. IEEE.

Kim YJ, Cheng S, Kim S and Iagnemma K (2013) A novel layer jamming mechanism with tunable stiffness capability for minimally invasive surgery. *IEEE Transactions on Robotics* 29(4): 1031–1042.

Langer M, Amanov E and Burgner-Kahrs J (2018) Stiffening sheaths for continuum robots. *Soft Robotics* 5(3): 291–303.

Mack C and Taylor HM (1956) 39—The fitting of woven cloth to surfaces. *Journal of the Textile Institute Transactions* 47(9): T477–T488.

Matsushita AK, Garcia LR, Liu ZK, Doan J, Meyers MA and McKittrick J (2020) Applying bio-inspired hierarchical design to jamming technology: Improving density-efficient mechanical properties and opening application

spaces. *Journal of Materials Research and Technology* 9(6): 15555–15565.

Mitsuda T and Matsuo N (2005) Shape stabilizer using an articulation-type passive element. *Proceedings of the JFPS International Symposium on Fluid Power* 2005(6): 723–727.

Mitsuda T, Kuge S, Wakabayashi M and Kawamura S (2002) Wearable force display using a particle mechanical constraint. *Presence* 11(6): 569–577.

Mitsuda T (2017) Variable-stiffness sheets obtained using fabric jamming and their applications in force displays. In: *2017 IEEE world haptics conference*, 6 June 2017, pp. 364–369. IEEE.

Mitsuda T, Wakabayashi M and Kawamura S (2003) Development of an upper-limb training orthosis using particle mechanical constraints. *Proceedings of the JSME Annual Conference on Robotics and Mechatronics* 2A1–3F–E3: 85.

Moriguchi S and Sato K (1972) Nunoji no kikagaku (Geometry of fabrics). In: *Sugaku Seminar*, Aug–Nov 1972, pp. 55–59.

Moriguchi S (1947) Furoshiki de suika wo tsutsumu hanashi (The story of wrapping a watermelon in a furoshiki). *The Applied Mathematics & the Applied Mechanics* 1(1): 47–48.

Narang YS, Vlassak JJ and Howe RD (2018) Mechanically versatile soft machines through laminar jamming. *Advanced Functional Materials* 28(17): 1707136.

Ou J, Yao L, Tauber D, Steimle J, Niiyama R and Ishii H (2014) jamSheets: Thin interfaces with tunable stiffness enabled by layer jamming. In: *Proceedings of the 8th international conference on tangible, embedded and embodied interaction*, February 2014, pp. 65–72.

Sadati SMH, Naghibi SE, Althoefer K and Nanayakkara T (2018) Toward a low hysteresis helical scale jamming interface inspired by teleost fish scale morphology and arrangement. In: *2018 IEEE international conference on soft robotics (RoboSoft)*, April 2018, pp. 455–460. IEEE.

Shah DS, Yang EJ, Yuen MC, Huang EC and Kramer-Bottiglio R (2021) Jamming skins that control system rigidity from the surface. *Advanced Functional Materials* 31(1): 2006915.

Shinohara A and Uchida S (1966) The surface fitness of textile fabrics. *Journal of the Textile Machinery Society of Japan* 19(1): 17–23.

Steltz E, Mozeika A, Rodenberg N, Brown E and Jaeger HM (2009) JSEL: Jamming skin enabled locomotion. In: *IEEE/RSJ international conference on intelligent robots and systems*, pp. 5672–5677. IEEE.

Wall V, Deimel R and Brock O (2015) Selective stiffening of soft actuators based on jamming. In: *2015 IEEE international conference on robotics and automation (ICRA)*, pp. 252–257. IEEE.

Zuo S, Iijima K, Tokumiya T and Masamune K (2014) Variable stiffness outer sheath with “dragon skin” structure and negative pneumatic shape-locking mechanism. *International Journal of Computer Assisted Radiology and Surgery* 9(5): 857–865.